Nov. 8, 2023

COL, a pipeline for identifying putatively functional back-splicing

Zhen Li[1], Fengyu Zhao[2], Tianjiao Zhou[3], Jianzhi Zhang[4,*] and Chuan Xu[1,*]

[1]Bio-X Institutes, Key Laboratory for the Genetics of Developmental and Neuropsychiatric Disorders, Ministry of Education, Shanghai Jiao Tong University, Shanghai 200240, China
[2]Department of Statistics, George Washington University, Washington, District of Columbia, DC 20052, USA.
[3]Department of Otorhinolaryngology Head and Neck Surgery, Shanghai Sixth People's Hospital Affiliated to Shanghai Jiao Tong University School of Medicine, Shanghai, 200233, China
[4]Department of Ecology and Evolutionary Biology, University of Michigan, Ann Arbor, MI 48109, USA

[*]Correspondence to
Jianzhi Zhang
Department of Ecology and Evolutionary Biology
University of Michigan
4018 Biological Sciences Building
1105 North University Avenue
Ann Arbor, MI 48109, USA
Phone: 734-763-0527
Email: jianzhi@umich.edu

Chuan Xu
Bio-X Institutes, Key Laboratory for the Genetics of Developmental and Neuropsychiatric Disorders, Ministry of Education
Shanghai Jiao Tong University
Shanghai 200240, China
Phone: 86-(0)21-34207976
Email: chuanx@sjtu.edu.cn

ABSTRACT

Circular RNAs (circRNAs) are a class of generally non-coding RNAs produced by back-splicing. Although the vast majority of circRNAs are likely to be products of splicing error and thereby confer no benefits to organisms, a small number of circRNAs have been found to be functional. Identifying other functional circRNAs from the sea of mostly non-functional circRNAs is an important but difficult task. Because available experimental methods for this purpose are of low throughput or versality and existing computational methods have limited reliability or applicability, new methods are needed. We hypothesize that functional back-splicing events that generate functional circRNAs (i) exhibit substantially higher back-splicing rates than expected from the total splicing amounts, (ii) have conserved splicing motifs, and (iii) show unusually high back-splicing levels. We confirm these features in back-splicing shared among human, macaque, and mouse, which should enrich functional back-splicing. Integrating the three features, we design a computational pipeline named COL for identifying putatively functional back-splicing. Using experimentally verified functional back-splicing as a benchmark, we find COL to outperform a commonly used computational method with a similar data requirement. We conclude that COL is an efficient and versatile method for rapid identification of putatively functional back-splicing and circRNAs that can be experimentally validated.

KEYWORDS

Functional circRNA, back-splicing rate, splicing motif, back-splicing level

INTRODUCTION

Circular RNAs (circRNAs) are a class of endogenous, single-stranded, covalently closed, mostly non-coding RNAs that are produced by back-splicing that links a downstream splice-donor site with an upstream splice-acceptor site [1, 2]. Over one half of human protein-coding genes produce circRNAs [3] and millions of circRNAs have been identified in animals [4] and human cancer cells [5, 6]. It is reported that circRNAs have important regulatory functions, such as acting as miRNA [7, 8] or protein [9] sponge to regulate gene expression, acting as scaffolds to mediate the formation of complexes [10], and being translated into small functional peptides [11, 12]. Additionally, a few circRNAs have been implicated in cardiovascular disease [13], Alzheimer's disease [14], cancer [6, 15, 16], and other diseases [17-19]. Notwithstanding, of millions of known circRNAs, those with demonstrated functions are a tiny fraction.

Our recent analysis of back-splicing in human, macaque, and mouse suggested that over 97% of back-splicing results from splicing error, supporting the error hypothesis of the origin of circRNAs and potentially explaining why only a tiny fraction of circRNAs have been found functional [20]. However, given the huge pool of circRNAs, it is reasonable to assume that not all functional circRNAs have been discovered. Identifying functional circRNAs is challenging because of the presence of orders of magnitude more nonfunctional circRNAs. One commonly used approach, which may be called the differential expression method (DEM) [21-23], detects differentially expressed circRNAs between two groups of samples (*e.g.*, patients vs. controls) and considers these circRNAs potentially functional. This method is obviously inapplicable to a single sample or non-comparable samples.

Another commonly used approach may be named the expression level method (ELM) [8, 24, 25]. It treats highly expressed circRNAs as putatively functional under the assumption that a circRNA needs to have a sufficiently high expression to exert its function. While functional circRNAs are likely to be highly expressed, highly expressed circRNAs may not be functional because their high expressions may simply arise from the high expressions of their parental genes. Hence, ELM is expected to generate many false positives when used alone for discovering functional circRNAs.

The conservation of circRNAs among species is another useful criterion for identifying functional circRNAs (referred to as the conservation method or CM), because random splicing errors are unlikely to be conserved across species [26-28]. However, CM requires not only the

sequenced genomes but also circRNA data from multiple species, hindering its wide application in non-model organisms.

In addition to the above three computational approaches, a high-throughput experimental screening method based on CRISPR-Cas13 was recently developed [29]. This experimental method greatly improves the discovery of functional circRNAs, but it is complicated and costly and cannot be used in species without a CRISPR-Cas13 screening system. Therefore, there is a need for a simple, inexpensive, and widely applicable method for identifying putatively functional circRNAs. In this work, we propose and validate such a method.

RESULTS

Three features of functional back-splicing

If a circRNA is functional, the back-splicing that generates the circRNA should be considered functional back-splicing. Therefore, to identify functional circRNAs is to discover functional back-splicing. Functional back-splicing is expected to have the following three features. First, the error hypothesis of the origin of circRNAs asserts that most back-splicing results from splicing error that is non-adaptive, predicting a negative correlation between the amount of splicing at a splicing junction and the back-splicing rate at the junction, which was indeed observed [20]. Functional back-splicing is expected to break this rule and have a higher back-splicing rate than predicted by the splicing amount. Second, functional back-splicing is expected to have conserved splicing motifs. Third, functional back-splicing should have a relatively high back-splicing level to allow the production of sufficient circRNA molecules.

To verify the above suggested characteristics of functional back-splicing empirically, we should ideally compare functional back-splicing with the rest of back-splicing. However, because only a few instances of back-splicing are demonstrably functional, we instead compared human back-splicing that is shared with macaque and mouse with human back-splicing that is unshared with these two species, because shared back-splicing is more likely than unshared back-splicing to be functional. Specifically, we first identified linearly spliced reads and back-spliced reads in appropriate RNA sequencing (RNA-seq) data from human, macaque, and mouse (see **Methods**). To reduce the impact of potential sequencing errors, we required at least two spliced reads to call a splicing event. We defined the total splicing amount at a splicing junction by the total number of spliced reads present in its donor and acceptor. Then, the back-splicing

rate at a back-splicing junction was computed by dividing the number of back-splicing reads by the total splicing amount at the junction (see **Methods**). To ensure the reliability in the discovery of shared back-splicing, we defined back-splicing as shared if it has at least two back-spliced reads in the same tissue in each of human, macaque, and mouse (see **Methods**); all other human back-splicing was regarded as unshared.

We started by analyzing back-splicing in human brain. Consistent with our previous finding [20], a significant negative correlation exists between the back-splicing rate and the total splicing amount across splicing junctions (**Fig. 1A**). To identify back-splicing violating this general rule, we regressed the back-splicing rate against the splicing amount (**Fig. 1A**) and calculated Cook's distance for each back-splicing event (see **Methods**). A back-splicing event is considered an outlier if its Cook's distance exceeds four times the mean Cook's distance of all back-splicing events (see **Methods**). We observed 1,377 outliers above and 281 outliers below the regression line, respectively (**Fig. 1A**). The error hypothesis predicts that the outliers above the regression line are beneficial (i.e., functional) whereas those below the regression line are particularly deleterious. Indeed, shared back-splicing contains significant more outliers above the regression line than does unshared back-splicing (**Fig. 1B**). By contrast, shared back-splicing contains fewer outliers below the regression line than does unshared back-splicing, although this difference is not statistically significant (**Fig. S1**).

Both linear-splicing and back-splicing use GU/AG splicing motifs. We found that the splicing motifs of 98.1% shared back-splicing are conserved, significantly higher than the corresponding value (74.5%) for unshared back-splicing ($P < 10^{-16}$, Fisher's exact test; **Fig. 1C**).

We then measured the relative back-splicing level at a splicing junction by the number of corresponding back-splicing reads per million total back-splicing reads in the sample (BSRPM) [30, 31]. Indeed, BSRPM is higher for shared than unshared back-splicing ($P < 10^{-13}$, Mann–Whitney U test; **Fig. 1D**).

Therefore, all three hypothesized features of functional back-splicing are verified in the shared back-splicing in the human brain. We repeated the above analyses in the other 10 tissues in the dataset and observed qualitatively similar results (**Fig. E-G**).

A feature-based integrative pipeline for identifying functional back-splicing

To examine the utility of the above three features for predicting shared (as a proxy for

functional) back-splicing, we measured the level of enrichment of shared back-splicing in the candidate back-splicing identified using these features. In the human brain, 1,484 (3.7%) of 39,687 back-splicing events are shared among human, macaque, and mouse; so, 3.7% is the baseline in our enrichment calculation. Of the 1,377 outliers over the regression line in **Fig. 1A**, 377 (or 27.4%) belong to shared back-splicing, a 7.4-fold enrichment relative to the baseline ($P < 10^{-16}$, Fisher's exact test; **Fig. 2A**). Similarly, 4.9% of back-splicing with conserved splicing motifs belong to shared back-splicing, a 1.32-fold enrichment relative to the baseline ($P < 10^{-16}$, Fisher's exact test; **Fig. 2A**). To compare the utility of back-splicing levels with that of regression outliers, we examined the top 1,377 back-splicing events in terms of their back-splicing levels and found that 26.7% of them belong to shared back-splicing, a 7.2-fold enrichment over the baseline ($P < 10^{-16}$, Fisher's exact test; **Fig. 2A**). Therefore, each of the three features alone has some power in predicting shared back-splicing.

We next examined whether a combination of the three features has an enhanced power in predicting shared back-splicing. We first used the Venn diagram to integrate the back-splicing events identified by each feature (**Fig. 2B**). We found that any combination of two features has a higher predictive power than any single feature. The combination of all three features has the highest power—34.9% of the 869 back-splicing events are shared (**Fig. 2B**).

While the above combination yields a set of candidates for shared back-splicing, it does not rank these candidates by their probabilities of sharing. To prioritize these candidates, we tested a few ordering methods such as Average, Stuart, and RRA that can integrate different ranking results [32] (see **Methods**). Because the feature of splicing motif conservation is binary (i.e., conserved or not), we only considered Cook's distance and back-splicing level in the ordering. Among the candidate back-splicing with all three features, the mean rank of shared back-splicing ordered by the RRA method is the smallest (smaller rankings mean higher probabilities of being shared) (**Fig. 2C**). Furthermore, in pairwise comparisons between the RRA ranking and any other ranking examined, more shared back-splicing events receive smaller RRA rankings (**Fig. 2D**). Therefore, the RRA method performs best in prioritizing the candidates for shared back-splicing.

Based on the above results from the analysis of shared back-splicing as a proxy for functional back-splicing, we developed an integrative pipeline to predict functional back-splicing (**Fig. 2E**). It first identifies outliers above the regression line between the back-splicing rate and

splicing amount across splicing junctions, then filters out those outliers without conserved splicing motifs, further filters out those without sufficiently high back-splicing levels, and finally prioritizes the candidates using RRA. Because this pipeline integrates conservation of splicing motifs, outliers in the regression analysis, and high back-splicing level, we refer to it as the COL method hereinafter.

Validating COL by functional back-splicing

In the above analyses, we used shared back-splicing as a proxy for functional back-splicing due to the scarcity of known functional back-splicing. Although shared back-splicing has a higher chance than average back-splicing to be functional, a more direct assessment of COL using functional back-splicing is warranted. Recently, a CRISPR-Cas13-mediated circRNA screen (CDCscreen) pipeline was developed by Li et al. to identify back-splicing necessary for cell proliferation [29]. Through this pipeline, 63, 62, and 67 candidate functional back-splicing events were found in Hela, 293FT, and HT29 cell lines, respectively (referred to as (CDCscreen-positive). The authors then randomly chose 9 candidates from each cell line in a knockdown experiment, confirming that 7, 8, 8 of them inhibited cell proliferation when knocked down (referred to as KD-validated). Below we used CDC-positive and KD-validated functional circRNAs to assess COL.

We first evaluated COL using the data from the Hela cell line. Using the same RNA-seq data used by Li et al. [29], we identified 6,369 back-splicing events with at least two supporting reads (see **Methods**), including 61 CDCscreen-positive and all 8 KO-validated functional back-splicing events. Using COL, we discovered 297 outliers over the regression line, among which 253 have conserved splicing motifs. The union of these 253 back-splicing events and the 253 back-splicing events with the highest back-splicing levels is a set of 190 candidate functional back-splicing events, which were then ranked by RRA. Among these 190 candidates, 25 are CDCscreen-positive (*i.e.*, a true positive rate of 41%) and seven are KD-validated (*i.e.*, a true positive rate of 87.5%; **Fig. 3A**). In 293FT and HT29 cell lines, COL respectively detected 28.1% and 21.2% of CDCscreen-positive back-splicing events and 57.1% and 50% of KD-validated back-splicing events (**Fig. 3A**).

We next compared the performance of COL with those of other methods. First, we randomly picked the same number of back-splicing events as identified by COL and examined

the numbers of CDCscreen-positive and KD-validated back-splicing events. This was repeated 1000 times to acquire the mean numbers. For example, we randomly picked 190 back-splicing events from Hela 1000 times but observed on average 1.65 CDCscreen-positive and 0.05 KD-validated back-splicing events, both of which are significantly smaller than those identified by COL ($P < 0.001$; **Fig. 3B**, **C**). Similar results were obtained in 293FT and HT29 (**Fig. 3B**, **C**).

We then compared COL with ELM, which is the only existing method that does not require more information than what COL uses. As mentioned, ELM detects putatively functional circRNAs by their high expressions. Because the back-splicing level, which is equivalent to the resulting circRNA expression level, is one of the three considerations of COL, COL should outperform ELM. This is indeed the case. For example, among the 190 back-splicing events with the highest back-splicing levels in Hela, 24 are CDCscreen-positive, fewer than the 25 identified by COL (**Fig. 3D**). Although the difference is small, this comparison is somewhat unfair to COL, because only 104 COL candidates but 114 ELM candidates were studied by CDCscreen. In 293FT and HT29, COL also identified more CDCscreen-positive back-splicing events than did ELM (**Fig. 3D**).

To further compare COL with ELM, we examined the rankings of the functional back-splicing candidates identified by the two methods (a smaller ranking indicates a higher probability of being functional). Of the 44 CDCscreen-positive back-splicing events identified by both methods from the three cell lines, 72.7% have smaller rankings in COL than ELM, significantly more than the random expectation of 50% ($P < 0.004$, binomial test; **Fig. 3E**), suggesting that COL performs better than ELM in rankings of putatively functional circRNAs identified.

Finally, we compared COL with ELM using KD-validated functional back-splicing. While the number of identified KD-validated back-splicing events is not significantly different between the two methods due to the small number of KD-validated events (**Fig. 3F**), 10 of 13 KD-validated events identified by both methods show smaller rankings by COL than by ELM (**Fig. 3G**), significantly more than the chance expectation ($P = 0.046$, binomial test).

DISCUSSION

Identifying the small fraction of millions of circRNAs that are potentially functional is a difficult task. In this study, we first demonstrated three features of functional back-splicing

(using back-splicing that is shared among human, macaque, and mouse as a proxy), and then developed the computational pipeline COL by considering and integrating the three features. We showed that COL outperforms random predictions and ELM in identifying functional back-splicing previously identified using CRISPR-Cas13 screening and knockdown validation. Unlike DEM that requires case and control samples, COL can be applied to a single sample. Compared with CM that depends on back-splicing data from multiple species, COL needs back-splicing data from only one species (plus genome sequences from other species).

The three features considered in COL have different predictive powers in identifying shared back-splicing. In particular, splicing motif conservation seems to be the least powerful feature (1.32-fold enrichment of shared back-splicing relative to the baseline), but when used together with another feature it can improve the predictive power of that feature. For example, the combination of regression outliers and splicing motif conservation achieves an 8.95-fold enrichment (**Fig. 2B**), which is even higher than the sum of the individual enrichments they bring (7.40 + 1.32 = 8.72, **Fig. 2A**).

Although the feature of regression outliers and the feature of high back-splicing levels bring similar levels of enrichment of shared back-splicing (**Fig. 2A**), the specific shared back-splicing they identify may not be similar. In fact, 83.8% of the candidates identified by one feature were also identified by the other feature (**Fig. S2A**). Of those candidates identified by one but not the other feature, more shared back-splicing events were found by the feature of regression outliers than by the feature of high back-splicing levels (**Fig. S2A**). Of the 333 shared back-splicing events identified by both features, the average rank of shared back-splicing is significantly smaller for the feature of regression outliers (ranked by RRA) than the feature of high back-splicing levels (ranked by the back-splicing level) (**Fig. S2B**). Furthermore, 62.2% of shared back-splicing has smaller ranks in the RRA ranking than in the back-splicing level ranking (**Fig. S2C**), significantly more than the random expectation of 50% ($P < 0.004$, binomial test). Therefore, the feature of regression outliers outperforms the feature of high back-splicing levels. The CDCscreen pipeline chooses back-splicing with the highest back-splicing levels for experimental screening [29]. Based on our results, using the feature of regression outliers or both features to select candidates for experimental screening would improve the efficiency of CDCscreen.

Apart from the three features considered in COL, functional back-splicing likely has

other properties. For example, back-splicing is regulated by *trans*-factors and *cis*-elements. Because *trans*-factors are the same for all back-splicing events in a cell whereas *cis*-elements are variable, the latter may be able to differentiate functional from non-functional back-splicing. Although COL already considers the conservation of splicing motifs, which are *cis*-elements, other *cis*-elements regulating back-splicing may be integrated in the pipeline in the future. For instance, complementary sequences in the intron adjacent to the splicing junction, especially Alu sequences, are key regulators mediating back-splicing [33-36]. However, due to the complexity of complementary sequences [33], it is not easy to evaluate their conservation among species. Therefore, we decided not to consider it at this stage.

Whether a back-splicing event is functional may also be inferred from the properties of its resultant circRNAs. Binding to miRNAs or proteins is presumably a main function of functional circRNAs [7, 8]. Thus, if the miRNA- or protein-binding motif in a circRNA is evolutionarily conserved, the circRNA and the corresponding back-splicing are likely functional. Indeed, some programs and webservers use binding information to predict circRNA functionality [37-39]. However, due to frequent alternative splicing inside circRNAs [40], the sequence and length of the circRNAs resulting from the same back-splicing are variable. The short reads from RNA-seq capture only back-spliced junctions and do not provide the whole circRNA sequence, hampering the consideration of binding motif conservation in COL. Because circRNAs can function through its protein products [11], translational activity would be another indicator of circRNA functionality. However, proteomic data are currently lacking in most studies, so the translation information is unavailable. These additional features may be integrated into COL when the relevant techniques become better or relevant data become available. However, we must caution that demonstrating a biochemical activity of a molecule (*e.g.*, binding to a protein or subject to translation) does not mean that the molecule has a biological function and the ultimate proof of the functionality of a molecule is that it is subject to selection [41].

METHODS

RNA-seq datasets

Our study requires datasets of both back-splicing and linear-splicing from the same sample. RNA-seq libraries enriched by oligo(dT) or treated by RNase R are inappropriate because the former filters out RNAs produced by back-splicing while the latter removes RNAs

generated by linear-splicing. Thus, we used RNA-seq data generated from total RNA samples treated with only the RiboMinus Kit because it removes rRNAs but retains both back-splicing and linear-splicing products. Specifically, the RiboMinus RNA-seq datasets from Ji P, et al. [3] downloaded from NGDC (https://ngdc.cncb.ac.cn/; ID: PRJCA000751) were used in our study. They include data from multiple tissues of human, macaque, and mouse. In addition, we used the RiboMinus RNA-seq datasets of HT29, 293FT, and Hela cell lines reported by Li S, et al. [29] and downloaded from GEO (https://www.ncbi.nlm.nih.gov/geo/; ID: GSE149691). All of the RNA-seq datasets were processed by FastQC to remove adaptors and bad reads by Trimmomatic and to filter out rRNAs through Bowtie alignment.

Linear-splicing and back-splicing

For the datasets from Ji P, et al. [3], linear-splicing and back-splicing junctions were retrieved following our previous study [20]. Briefly, we used the genome assemblies of GRCh38 for human, Mmul 8.0.1 for macaque, and GRCm38 for mouse, all downloaded with gene annotations from Ensembl release 89. Linear-splicing was inferred by Tophat2 [42] using default parameters, including annotated and newly identified splicing. Back-splicing was identified by CIRCexplorer2 [33], which was then merged with newly identified back-splicing by CIRI2 [43, 44].

Li S, et al. [29] analyzed their data using GRCh37. To be consistent with their results, we analyzed their data using the same human genome reference (Ensemble release 75). Specifically, linear-splicing was identified by STAR (v2.4.2) using default parameters. We followed the original authors to identify back-splicing. That is, HISAT2 was used to map clean reads to the reference genome; the unmapped reads were collected by Samtools and further mapped to the reference genome by TopHat-Fusion. Finally, CIRCexploere2 was used for parsing back-splicing from the mapping results of TopHat-Fusion.

Splicing amount, back-splicing rate, and back-splicing level

A splicing event has an acceptor site and a donor site. The total splicing amount at a splicing junction is the total number of linear- and back-splicing reads of its acceptor and donor sites. The back-splicing rate is twice the number of back-spliced reads divided by the total splicing amount at the back-splicing junction (**Fig. S3**). The relative back-splicing level at a

back-spliced junction is the number of back-spliced reads at the junction per million total back-spliced reads in the sample (BSRPM).

Cook's distance

Cook's distance is used in regression analysis to find influential outliers [45]. The formula for calculating Cook's distance of data point i is $D_i = \frac{\sum_{j=1}^{n}[\hat{y}_j - \hat{y}_{j(i)}]^2}{p \times MSE}$, where $\hat{y}_j$ is the jth data point's fitted response value, $\hat{y}_{j(i)}$ is the jth data point's fitted response value when data point i is removed, n is the number of data points, MSE is the mean squared error of the regression model, and p is the number of coefficients in the regression model. Four times the mean Cook's distance of all data points was used as the cutoff to call outlies in our study. The commonly used cutoff advised by statistical tools R [46] and MATLAB [47] is three times. We used a stricter cutoff to guard against false positives.

Ordering of back-splicing events

Back-splicing events were ordered using several different methods, including Average, Robust Rank Aggregation (RRA) [32], and Stuart [48]. The Average method simply takes the mean of the ranks of a target from multiple samples. RRA and Stuart are both based on order statistics in rank aggregation, but the former is more robust than the latter to noise [32]. All orderings were executed by the R package RobustRankAggreg. In addition, back-splicing events were ordered by their Cook's distances or back-splicing levels.

Splicing motif conservation and shared back-splicing

Back-splicing motifs, same as the linear-splicing motifs, are GU adjacent to the donor site and AG adjacent to the acceptor site. We used the LiftOver (http://genome.ucsc.edu/cgi-bin/hgLiftOver) to identify the orthologous genomic loci across species. If the nucleotides of a back-splicing motif in one species are the same as the nucleotides of the orthologous locus in another species, this motif is conserved; otherwise, it is unconserved.

If a back-splicing event in one species is also observed at the orthologous locus of another species, the back-splicing event is considered shared between the two species. In this study, shared back-splicing refers to back-splicing events shared among human, macaque, and

mouse.

Data visualization and statistical analyses

R (v3.5.1) was used in statistical analyses and data visualization. Figures were generated using R packages, including ggplot2 and its dependencies.

ACKNOWLEDGEMENTS

We thank Dr. Wei Xue for his help in processing the data from Li et al (2021). This study was supported by National Natural Science Foundation of China (32270704 and 32100518), National Science and Technology Innovation 2030 Major Projects for 'Brain Science and Brain-Inspired Research' (2022ZD0214400), Medical-Engineering Crossover Fund of Shanghai Jiao Tong University (YG2022QN084), and the U.S. National Institutes of Health (grant R35GM139484 to J.Z.).

AUTHOR CONTRIBUTIONS

C.X. and J.Z. conceived the study and wrote the paper. Z.L., C.X., F.Z., T.Z performed the study and analyzed the data.

REFERENCES

1. Kristensen LS, Andersen MS, Stagsted LVW, Ebbesen KK, Hansen TB, Kjems J: **The biogenesis, biology and characterization of circular RNAs.** *Nat Rev Genet* 2019, **20:**675-691.
2. Chen LL: **The biogenesis and emerging roles of circular RNAs.** *Nat Rev Mol Cell Bio* 2016, **17:**205-211.
3. Ji P, Wu W, Chen S, Zheng Y, Zhou L, Zhang J, Cheng H, Yan J, Zhang S, Yang P, Zhao F: **Expanded Expression Landscape and Prioritization of Circular RNAs in Mammals.** *Cell Rep* 2019, **26:**3444-3460 e3445.
4. Wu W, Ji P, Zhao F: **CircAtlas: an integrated resource of one million highly accurate circular RNAs from 1070 vertebrate transcriptomes.** *Genome Biol* 2020, **21:**101.
5. Feng J, Chen W, Dong X, Wang J, Mei X, Deng J, Yang S, Zhuo C, Huang X, Shao L, et al: **CSCD2: an integrated interactional database of cancer-specific circular RNAs.** *Nucleic Acids Res* 2022, **50:**D1179-D1183.
6. Vo JN, Cieslik M, Zhang Y, Shukla S, Xiao L, Zhang Y, Wu YM, Dhanasekaran SM, Engelke CG, Cao X, et al: **The Landscape of Circular RNA in Cancer.** *Cell* 2019, **176:**869-881 e813.
7. Hansen TB, Jensen TI, Clausen BH, Bramsen JB, Finsen B, Damgaard CK, Kjems J: **Natural RNA circles function as efficient microRNA sponges.** *Nature* 2013, **495:**384-388.

8. Memczak S, Jens M, Elefsinioti A, Torti F, Krueger J, Rybak A, Maier L, Mackowiak SD, Gregersen LH, Munschauer M, et al: **Circular RNAs are a large class of animal RNAs with regulatory potency.** *Nature* 2013, **495:**333-338.
9. Ashwal-Fluss R, Meyer M, Pamudurti NR, Ivanov A, Bartok O, Hanan M, Evantal N, Memczak S, Rajewsky N, Kadener S: **circRNA biogenesis competes with pre-mRNA splicing.** *Mol Cell* 2014, **56:**55-66.
10. Du WW, Yang W, Liu E, Yang Z, Dhaliwal P, Yang BB: **Foxo3 circular RNA retards cell cycle progression via forming ternary complexes with p21 and CDK2.** *Nucleic Acids Res* 2016, **44:**2846-2858.
11. Pamudurti NR, Bartok O, Jens M, Ashwal-Fluss R, Stottmeister C, Ruhe L, Hanan M, Wyler E, Perez-Hernandez D, Ramberger E, et al: **Translation of CircRNAs.** *Mol Cell* 2017, **66:**9-21 e27.
12. Legnini I, Di Timoteo G, Rossi F, Morlando M, Briganti F, Sthandier O, Fatica A, Santini T, Andronache A, Wade M, et al: **Circ-ZNF609 Is a Circular RNA that Can Be Translated and Functions in Myogenesis.** *Molecular Cell* 2017, **66:**22-+.
13. Aufiero S, Reckman YJ, Pinto YM, Creemers EE: **Circular RNAs open a new chapter in cardiovascular biology.** *Nat Rev Cardiol* 2019, **16:**503-514.
14. Song CH, Zhang YF, Huang WY, Shi JY, Huang Q, Jiang MJ, Qiu Y, Wang T, Chen HZA, Wang H: **Circular RNA Cwc27 contributes to Alzheimer's disease pathogenesis by repressing Pur-alpha activity.** *Cell Death Differ* 2022, **29:**393-406.
15. Kristensen LS, Hansen TB, Veno MT, Kjems J: **Circular RNAs in cancer: opportunities and challenges in the field.** *Oncogene* 2018, **37:**555-565.
16. Meng SJ, Zhou HC, Feng ZY, Xu ZH, Tang Y, Li PY, Wu MH: **CircRNA: functions and properties of a novel potential biomarker for cancer.** *Molecular Cancer* 2017, **16**.
17. Holdt LM, Stahringer A, Sass K, Pichler G, Kulak NA, Wilfert W, Kohlmaier A, Herbst A, Northoff BH, Nicolaou A, et al: **Circular non-coding RNA ANRIL modulates ribosomal RNA maturation and atherosclerosis in humans.** *Nature Communications* 2016, **7**.
18. Stoll L, Sobel J, Rodriguez-Trejo A, Guay C, Lee K, Veno MT, Kjems J, Laybutt DR, Regazzi R: **Circular RNAs as novel regulators of beta-cell functions in normal and disease conditions.** *Mol Metab* 2018, **9:**69-83.
19. Lei KX, Bai HT, Wei ZH, Xie CQ, Wang JK, Li J, Chen QM: **The mechanism and function of circular RNAs in human diseases.** *Exp Cell Res* 2018, **368:**147-158.
20. Xu C, Zhang J: **Mammalian circular RNAs result largely from splicing errors.** *Cell Rep* 2021, **36:**109439.
21. Guo JN, Li J, Zhu CL, Feng WT, Shao JX, Wan L, Huang MD, He JD: **Comprehensive profile of differentially expressed circular RNAs reveals that hsa_circ_0000069 is upregulated and promotes cell proliferation, migration, and invasion in colorectal cancer.** *Oncotargets Ther* 2016, **9:**7451-7458.
22. Huang MG, Zhong ZY, Lv MX, Shu J, Tian Q, Chen JX: **Comprehensive analysis of differentially expressed profiles of lncRNAs and circRNAs with associated co-expression and ceRNA networks in bladder carcinoma.** *Oncotarget* 2016, **7:**47186-47200.
23. Reiner A, Yekutieli D, Benjamini Y: **Identifying differentially expressed genes using false discovery rate controlling procedures.** *Bioinformatics* 2003, **19:**368-375.
24. Huang X, He M, Huang S, Lin RR, Zhan M, Yang D, Shen H, Xu SW, Cheng W, Yu JX, et al: **Circular RNA circERBB2 promotes gallbladder cancer progression by regulating**

PA2G4-dependent rDNA transcription. *Molecular Cancer* 2019, **18**.
25. Zhang D, Ni N, Wang Y, Tang Z, Gao H, Ju Y, Sun N, He X, Gu P, Fan X: **CircRNA-vgll3 promotes osteogenic differentiation of adipose-derived mesenchymal stem cells via modulating miRNA-dependent integrin alpha5 expression.** *Cell Death Differ* 2021, **28:**283-302.
26. Rybak-Wolf A, Stottmeister C, Glazar P, Jens M, Pino N, Giusti S, Hanan M, Behm M, Bartok O, Ashwal-Fluss R, et al: **Circular RNAs in the Mammalian Brain Are Highly Abundant, Conserved, and Dynamically Expressed.** *Molecular Cell* 2015, **58:**870-885.
27. Suenkel C, Cavalli D, Massalini S, Calegari F, Rajewsky N: **A Highly Conserved Circular RNA Is Required to Keep Neural Cells in a Progenitor State in the Mammalian Brain.** *Cell Reports* 2020, **30:**2170-2179.
28. Heumuller AW, Jones AN, Mourao A, Klangwart M, Shi CY, Wittig I, Fischer A, Muhly-Reinholz M, Buchmann GK, Dieterich C, et al: **Locus-Conserved Circular RNA cZNF292 Controls Endothelial Cell Flow Responses.** *Circ Res* 2022, **130:**67-79.
29. Li S, Li X, Xue W, Zhang L, Yang LZ, Cao SM, Lei YN, Liu CX, Guo SK, Shan L, et al: **Screening for functional circular RNAs using the CRISPR-Cas13 system.** *Nat Methods* 2021, **18:**51-59.
30. Liu Z, Ran Y, Tao C, Li S, Chen J, Yang E: **Detection of circular RNA expression and related quantitative trait loci in the human dorsolateral prefrontal cortex.** *Genome Biol* 2019, **20:**99.
31. Okholm TLH, Sathe S, Park SS, Kamstrup AB, Rasmussen AM, Shankar A, Chua ZM, Fristrup N, Nielsen MM, Vang S, et al: **Transcriptome-wide profiles of circular RNA and RNA-binding protein interactions reveal effects on circular RNA biogenesis and cancer pathway expression.** *Genome Med* 2020, **12:**112.
32. Kolde R, Laur S, Adler P, Vilo J: **Robust rank aggregation for gene list integration and meta-analysis.** *Bioinformatics* 2012, **28:**573-580.
33. Zhang XO, Wang HB, Zhang Y, Lu X, Chen LL, Yang L: **Complementary sequence-mediated exon circularization.** *Cell* 2014, **159:**134-147.
34. Ivanov A, Memczak S, Wyler E, Torti F, Porath HT, Orejuela MR, Piechotta M, Levanon EY, Landthaler M, Dieterich C, Rajewsky N: **Analysis of intron sequences reveals hallmarks of circular RNA biogenesis in animals.** *Cell Rep* 2015, **10:**170-177.
35. Wilusz JE: **Repetitive elements regulate circular RNA biogenesis.** *Mob Genet Elements* 2015, **5:**1-7.
36. Jeck WR, Sorrentino JA, Wang K, Slevin MK, Burd CE, Liu J, Marzluff WF, Sharpless NE: **Circular RNAs are abundant, conserved, and associated with ALU repeats.** *RNA* 2013, **19:**141-157.
37. Dudekula DB, Panda AC, Grammatikakis I, De S, Abdelmohsen K, Gorospe M: **CircInteractome: A web tool for exploring circular RNAs and their interacting proteins and microRNAs.** *RNA Biol* 2016, **13:**34-42.
38. Deng L, Lin W, Wang J, Zhang J: **DeepciRGO: functional prediction of circular RNAs through hierarchical deep neural networks using heterogeneous network features.** *BMC Bioinformatics* 2020, **21:**519.
39. Cardenas J, Balaji U, Gu J: **Cerina: systematic circRNA functional annotation based on integrative analysis of ceRNA interactions.** *Sci Rep* 2020, **10:**22165.
40. Zhang XO, Dong R, Zhang Y, Zhang JL, Luo Z, Zhang J, Chen LL, Yang L: **Diverse alternative back-splicing and alternative splicing landscape of circular RNAs.**

Genome Res 2016, **26:**1277-1287.
41. Graur D, Amy K S, Tim F. C.: *Molecular and genome evolution.* Massachusetts, USA: Sinauer Associates, Inc.; 2016.
42. Kim, Geo Pertea, Cole Trapnell, Harold Pimentel, Ryan Kelley, Salzberg SL: **TopHat2: accurate alignment of transcriptomes in the presence of insertions, deletions and gene fusions.** *Genome Biol* 2013.
43. Gao Y, Wang J, Zhao F: **CIRI: an efficient and unbiased algorithm for de novo circular RNA identification.** *Genome Biol* 2015, **16:**4.
44. Gao Y, Zhang J, Zhao F: **Circular RNA identification based on multiple seed matching.** *Brief Bioinform* 2018, **19:**803-810.
45. Cook RD: **Detection of Influential Observation in Linear Regression.** *TECHNOMETRICS* 1977, **19**.
46. **https://rpubs.com/DragonflyStats/Cooks-Distance.**
47. **https://www.mathworks.com/help/stats/cooks-distance.html.**
48. Stuart JM, Segal E, Koller D, Kim SK: **A gene-coexpression network for global discovery of conserved genetic modules.** *Science* 2003, **302:**249-255.

Figure and legends

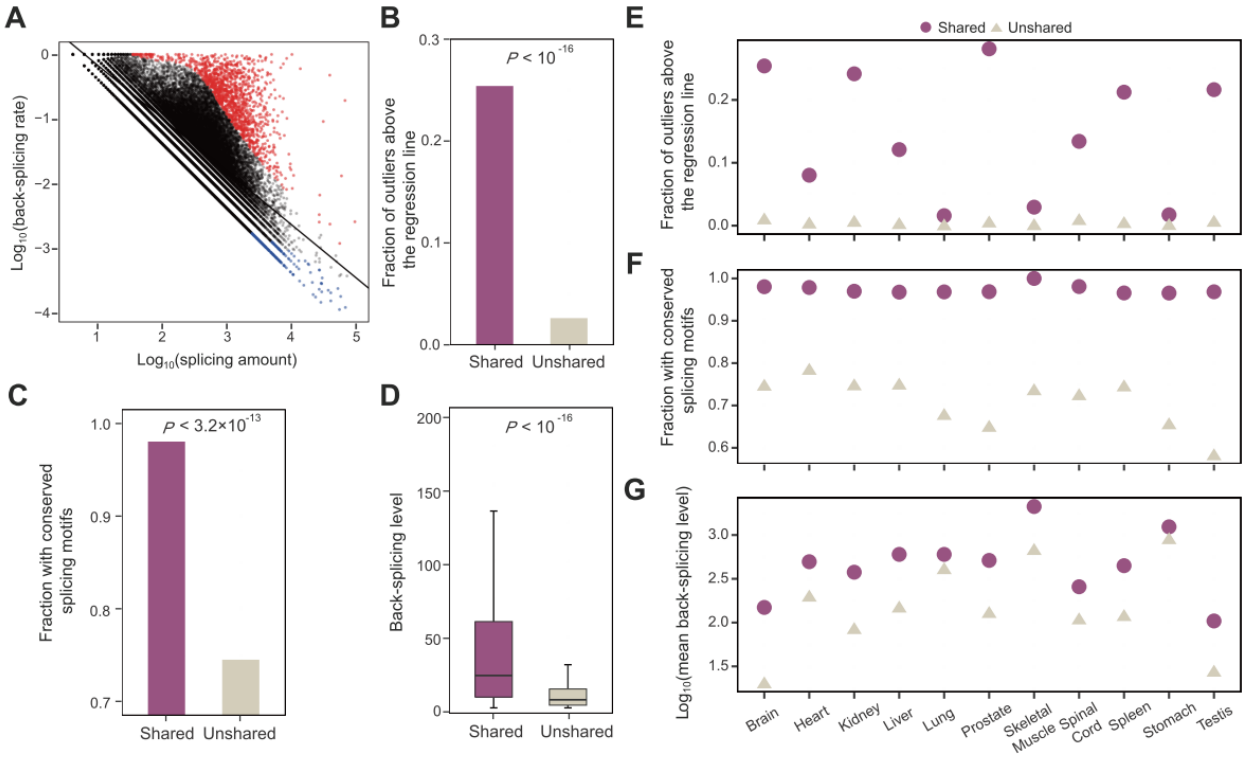

Fig. 1. Comparison of three features in shared and unshared back-splicing in various human tissues. (**A**) Linear regression between the back-splicing rate and splicing amount across back-splicing junctions. Each dot represents a back-splicing junction, and the solid black line shows the linear least-squares regression. Red and blue dots are outliers above and below the regression line, respectively. (**B**) Outliers above the regression line are enriched in shared back-splicing relative to unshared back-splicing. (**C**) Shared back-splicing has a higher fraction of conserved splicing motifs than does unshared back-splicing. (**D**) The back-splicing level is higher for shared than unshared back-splicing. Data in (A) to (D) are from the brain. **(E-G)** Comparison of the three features between shared and unshared back-splicing across 11 human tissues. In (D) and (G), the back-splicing level at a back-splicing junction is measured by the number of back-spliced reads at the junction per million total back-spliced reads in the sample (BSRPM).

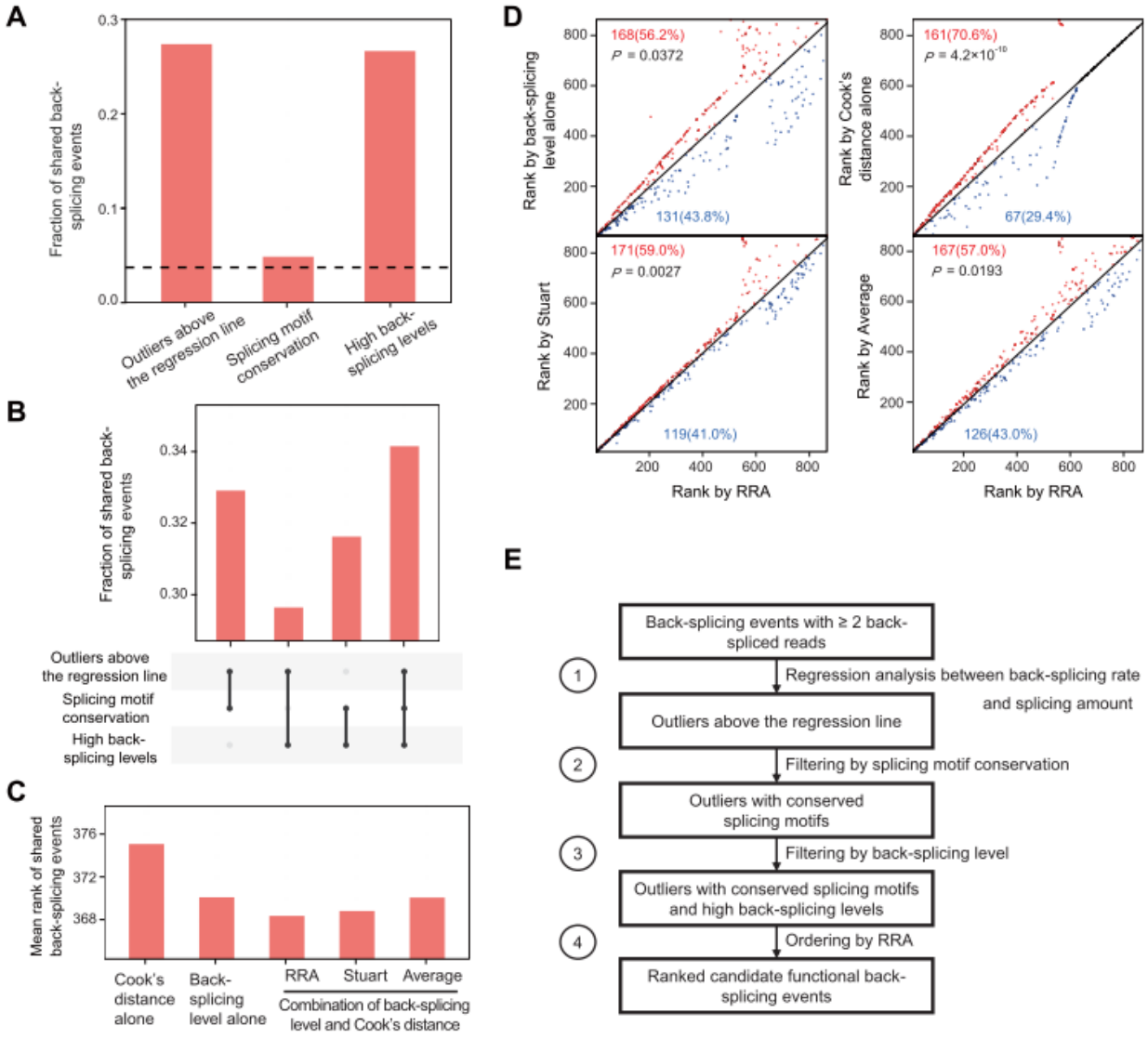

Fig. 2. Predicting shared back-splicing using combinations of the three features. (**A**) The prediction power of each feature. (**B**) The prediction power of combined features through Venn diagram integration. (**C**) Mean rank of shared back-splicing according to different ordering methods. Smaller ranks mean higher probabilities of being shared. (**D**) Pairwise comparison between RRA ranking and four other rankings. Each dot represents a back-splicing event. Dots above and below the diagonal are respectively colored in blue and red, with their numbers and fractions indicated. *P*-values are from binomial tests. (**E**) The integrative pipeline of COL for predicting functional back-splicing.

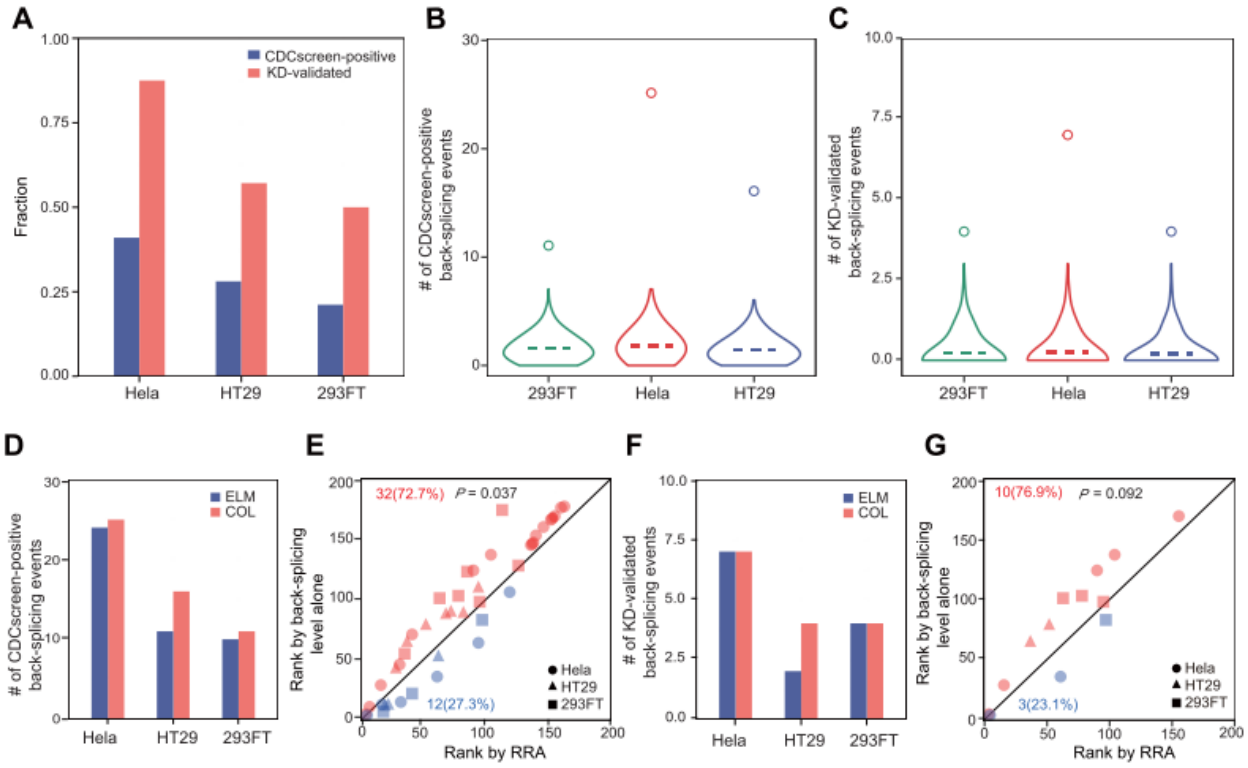

Fig. 3. Performance of COL in identified functional circRNAs in cell lines Hela, HT29 and 293FT. (**A**) Fraction of CDCscreen-positive or KD-validated back-splicing events identified by COL. (**B-C**) Numbers of CDCscreen-positive (**B**) and KD-validated (**C**) back-splicing events identified by COL (circles) or randomization (violin plots). Each violin plot shows the result of 1000 random simulations with the dash line indicating the mean. (**D**) Number of CDCscreen-positive back-splicing events identified by COL or ELM. (**E**) Ranks of CDCscreen-positive back-splicing events. Putatively functional back-splicing events identified by COL are ranked by RRA whereas those identified by ELM are ranked by the back-splicing level. Dots above and below the diagonal are respectively colored in red and blue, with their numbers and fractions indicated. Binomial *P*-value is presented. (**F**) Number of KD-validated functional back-splicing events identified by COL or ELM. (**G**) Ranks of KD-validated functional back-splicing events.

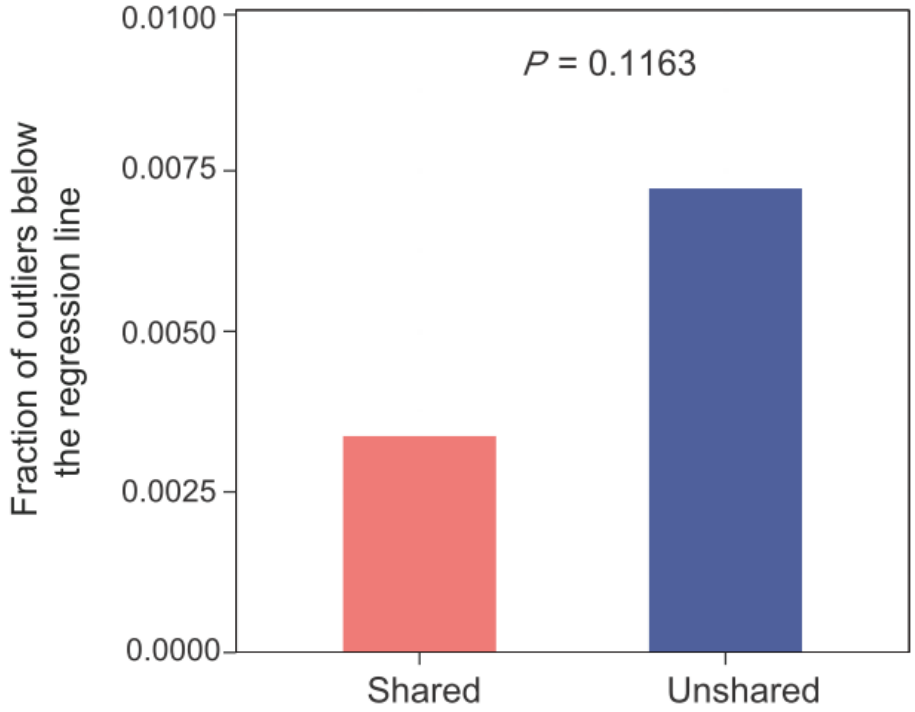

Fig. S1. There is no significant difference between shared and unshared back-splicing in their fraction of outliers below the regression line.

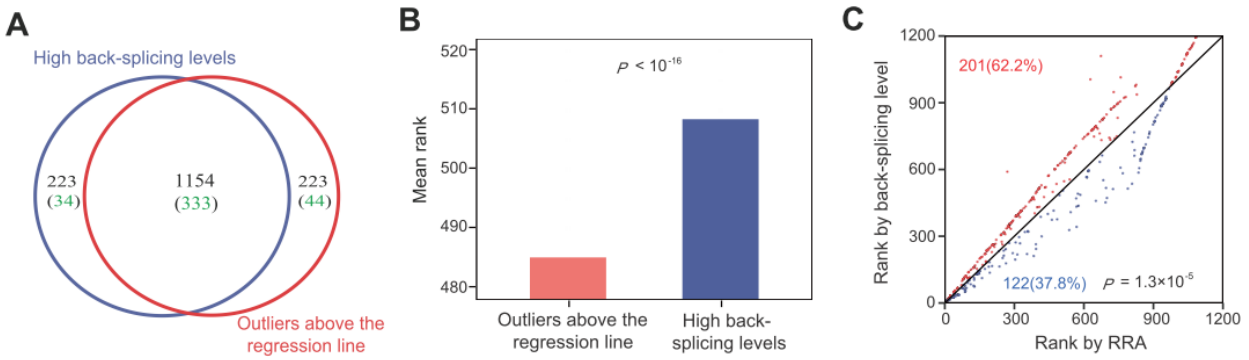

Fig. S2. Comparison in prediction power between two features: outliers above the regression line and high back-splicing levels. (**A**) The Venn diagram of back-splicing events identified by the two features. Black and green numbers represent the number of identified back-splicing events and the number of shared back-splicing events, respectively. (**B**) Mean rank of the 333 shared back-splicing events identified by both features. (**C**) Ranks of the shared back-splicing events by two ordering methods. Each dot represents a back-splicing event, where the Y-axis indicates its rank according to the back-splicing level while the X-axis indicates its RRA rank by the feature of regression outliers. Dots above and below the diagonal are respectively colored in red and blue, with their numbers and fractions indicated. Binomial *P*-value is presented.

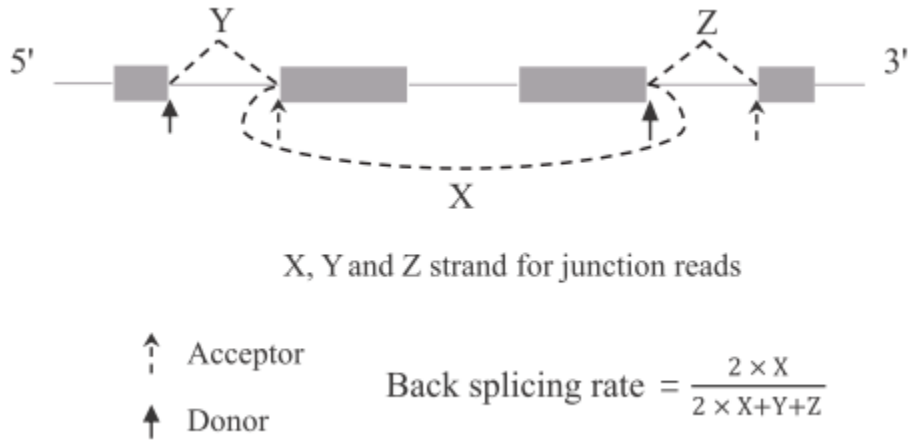

Fig. S3. Diagram explaining the calculation of the back-splicing rate at a back-splicing junction.